ADVANCED MATERIALS
www.advmat.de

Printable Skin-Driven Mechanoluminescence Devices via Nanodoped Matrix Modification

Xin Qian, Zheren Cai, Meng Su, Fengyu Li, Wei Fang, Yudong Li, Xue Zhou, Qunyang Li, Xiqiao Feng, Wenbo Li, Xiaotian Hu, Xiandi Wang, Caofeng Pan, and Yanlin Song**

Mechanically driven light generation is an exciting and under-exploited phenomenon with a variety of possible practical applications. However, the current driving mode of mechanoluminescence (ML) devices needs strong stimuli. Here, a flexible sensitive ML device via nanodopant elasticity modulus modification is introduced. Rigid ZnS:M^{2+}(Mn/Cu)@Al_2O_3 microparticles are dispersed into soft poly(dimethylsiloxane) (PDMS) film and printed out to form flexible devices. For various flexible and sensitive scenes, SiO_2 nanoparticles are adopted to adjust the elasticity modulus of the PDMS matrix. The doped nanoparticles can concentrate stress to ZnS:M^{2+}(Mn/Cu)@Al_2O_3 microparticles and achieve intense ML under weak stimuli of the moving skin. The printed nano-/microparticle-doped matrix film can achieve skin-driven ML, which can be adopted to present fetching augmented animations expressions. The printable ML film, amenable to large areas, low-cost manufacturing, and mechanical softness will be versatile on stress visualization, luminescent sensors, and open definitely new functional skin with novel augmented animations expressions, the photonic skin.

Electronic skin (E-skin) has contributed to the development of smart sensors,[1] biomedical diagnostics,[2] wearable devices,[3] robotics,[4] and flexible electronics.[5] This progress is hysteretic on luminescence functionalization. Piezoelectrically induced electron detrapping electrofluorescence of inorganic hybrid semiconductors (ZnS:M^{2+}(Mn/Cu), $SrAl_2O_4$:Eu, SrAl4O6:Eu, etc.) contributes actually mechanoluminescence (ML) phenomenon.[6–9] However, the poly(dimethylsiloxane) (PDMS)-supported rigid inorganic hybrid semiconductor phosphors can barely luminescence with weak stimuli because soft or flexible matrix acts as stress buffer.[10–12] In fact, the matched combination of various hardness materials is a critical challenge for flexible device mechanics, particularly, multimaterial composition and multifunctional integration devices.[13] Although many works focus on synthesis and chemical component of ML materials,[14] but the mechanics of stress transfer from matrix to ML particles is neglected, which contains the more general adoptability for devices. Here, we demonstrated a flexible sensitive ML device via nanodopant elasticity modulus modification of matrix. Rigid ZnS:M^{2+}(Mn/Cu)@Al_2O_3 microparticles (ZMPs) were dispersed into soft PDMS film and printed out to form flexible devices. SiO_2 nanoparticles were adopted to adjust the elasticity modulus of PDMS matrix for various flexible and sensitive scenes. The doped SiO_2 nanoparticles can concentrate stress to ZMPs and achieve intense ML under weak stimuli. We demonstrated the relationship between the elastic modulus of polymer matrix

X. Qian, Z. Cai, Dr. M. Su, Prof. F. Li, Y. Li, X. Zhou, Dr. W. Li, X. T. Hu, Prof. Y. Song
Key Laboratory of Green Printing
CAS Research/Education Center for Excellence in Molecular Sciences
Institute of Chemistry
Chinese Academy of Sciences (ICCAS)
Beijing Engineering Research Center of Nanomaterials for Green Printing Technology
National Laboratory for Molecular Sciences (BNLMS)
Beijing 100190, P. R. China
E-mail: forrest@iccas.ac.cn; ylsong@iccas.ac.cn
X. Qian, Z. Cai, X. T. Hu
University of Chinese Academy of Sciences
Beijing 100049, P. R. China

The ORCID identification number(s) for the author(s) of this article can be found under https://doi.org/10.1002/adma.201800291.

DOI: 10.1002/adma.201800291

W. Fang, Prof. Q. Li, Prof. X. Feng
Department of Engineering Mechanics
AML
Tsinghua University
Beijing 100084, P. R. China
W. Fang, Prof. X. Feng
Department of Engineering Mechanics
Institute of Biomechanics and Medical Engineering
Tsinghua University
Beijing 100084, P. R. China
Prof. Q. Li
Center for Nano and Micro Mechanics
Tsinghua University
Beijing 100084, P. R. China
Dr. X. Wang, Prof. C. Pan
Beijing Institute of Nanoenergy and Nanosystems
Chinese Academy of Sciences
Beijing 100083, P. R. China

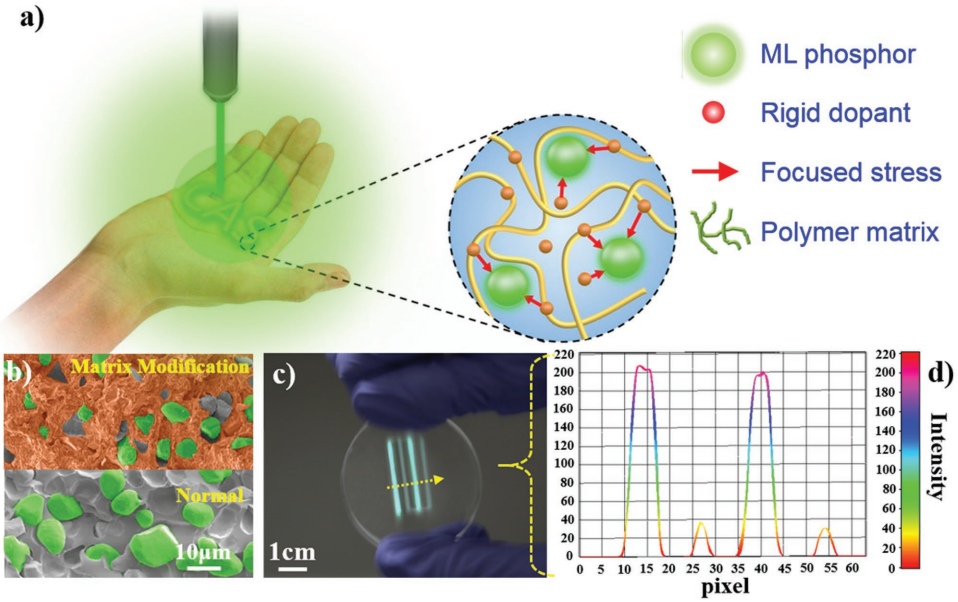

Figure 1. Nanodoped matrix modification for sensitive ML and printable devices. a) The schematic illustration of sensitive ZMPs ML by nanoparticle-doped matrix. b) SEM images of the micro (10–30 μm) ZMPs ML matrix with/without SiO_2 nanoparticle doping. c) The ML intensity contrast of matrix modification. d) ML intensity along the arrow obtained by analyzing the photo (c).

and ML performance by finite element analysis (FEA). The printable ML film, amenable to large areas, low-cost manufacturing, and mechanical softness will be versatile on stress visualization, luminescent sensors,[15–19] and open definitely new functional skin with novel augmented animations expressions, the photonic skin.[11]

ZMPs serve as ML materials, which luminesce when adopted stress. Through a two-way coupling effect between piezoelectricity and photoexcitation property, piezophotonic effect triggers the conversion from mechanical stress to visible light emission, i.e., the ML process.[20] Elastic matrix (PDMS, etc.) can transmit stress or stretch to embedded ZMPs and trigger flexible ML.[21] However, the elastic deformation of flexible materials buffers the stress or stretch which acts on rigid phosphor microparticles and cannot trigger abundant electron detrapping and obvious ML. As schemed in **Figure 1**a, we introduced SiO_2 nanoparticles into PDMS matrix. The SiO_2 nanoparticles can be completely wetted and closely adhered by PDMS macromolecular chains. Scanning electron microscopy (SEM) images in Figure 1b and Figure S3 in the Supporting Information display that SiO_2 nanoparticles were uniformly dispersed in PDMS matrix. Because of the formation of —O—Si— chemical bonds, the adhesion of SiO_2 and Al_2O_3 with PDMS is much stronger than other materials.[22] The strong adhesion guarantees our devices to exhibit high performance and durability.[23] Figure 1c shows distinct luminescence of ZMPs patterns printed in PDMS membrane with/without SiO_2 nanoparticle doping under hands stretch. Figure 1d presents that there is five times ML intensity enhancement of the SiO_2 nanoparticle doping one.

Correspondence of ML intensity to strain, elastic modulus, doping nanoparticle size, or concentration was investigated. **Figure 2**a presents a quadratic relation of the ML intensity (normalized intensity) and strain, when the matrix elastic modulus is 1 MPa, and strain varies from 5% to 30%. The ML intensity exhibits an approximately quadratic to the elastic modulus of polymer matrix, with fixed 10% strain, as Figure 2b. Movies S1 and S2 in the Supporting Information show devices working under different strain levels and different elastic modulus. The maximum principal stress is proportional to the strain of film and the elastic modulus of matrix.[24] We concluded the relationship of ML intensity to strain and elastic modulus by following equation

$$I = \mathrm{A}\, E^2\, \varepsilon^2 \tag{1}$$

I is the ML intensity, E is the elastic modulus, and ε is strain. A is a constant calculated from experimental data. (More details in Figure S6d, Supporting Information).

The serial experiments of doped SiO_2 nanoparticle size, the ratio-defined luminescence sensitivity, and elastic modulus were processed to investigate the doping scale effect. As Figure 2c shown, the ML intensity rapidly increases during doped SiO_2 nanoparticle size from 10–100 nm[25,26] and slowly decreases during 100–500 nm. Figure 2d illustrates that the elastic modulus has the same tendency corresponding to doped scale effect and concentration. In most cases, composite film with high elastic modulus has high luminescence intensity. As for matrix's elastic modulus, it is proportional to doping concentration.[23,27] Luminescence intensity begins to decline when the doping concentration is greater than 25 wt%, which could be ascribed to the light scattering. When doping concentration is greater than 25 wt%, the increased particle density will block and scatter the luminescence. For the 10 μm ZMPs phosphors, 100 nm SiO_2 nanoparticles doping results the highest elastic modulus. With the same doping weight ratio, the increase of doped nanoparticle size results the decrease of doped particle amount which attributes to the decrease of active point amount between doped nanoparticles and ZMPs. However, when doped

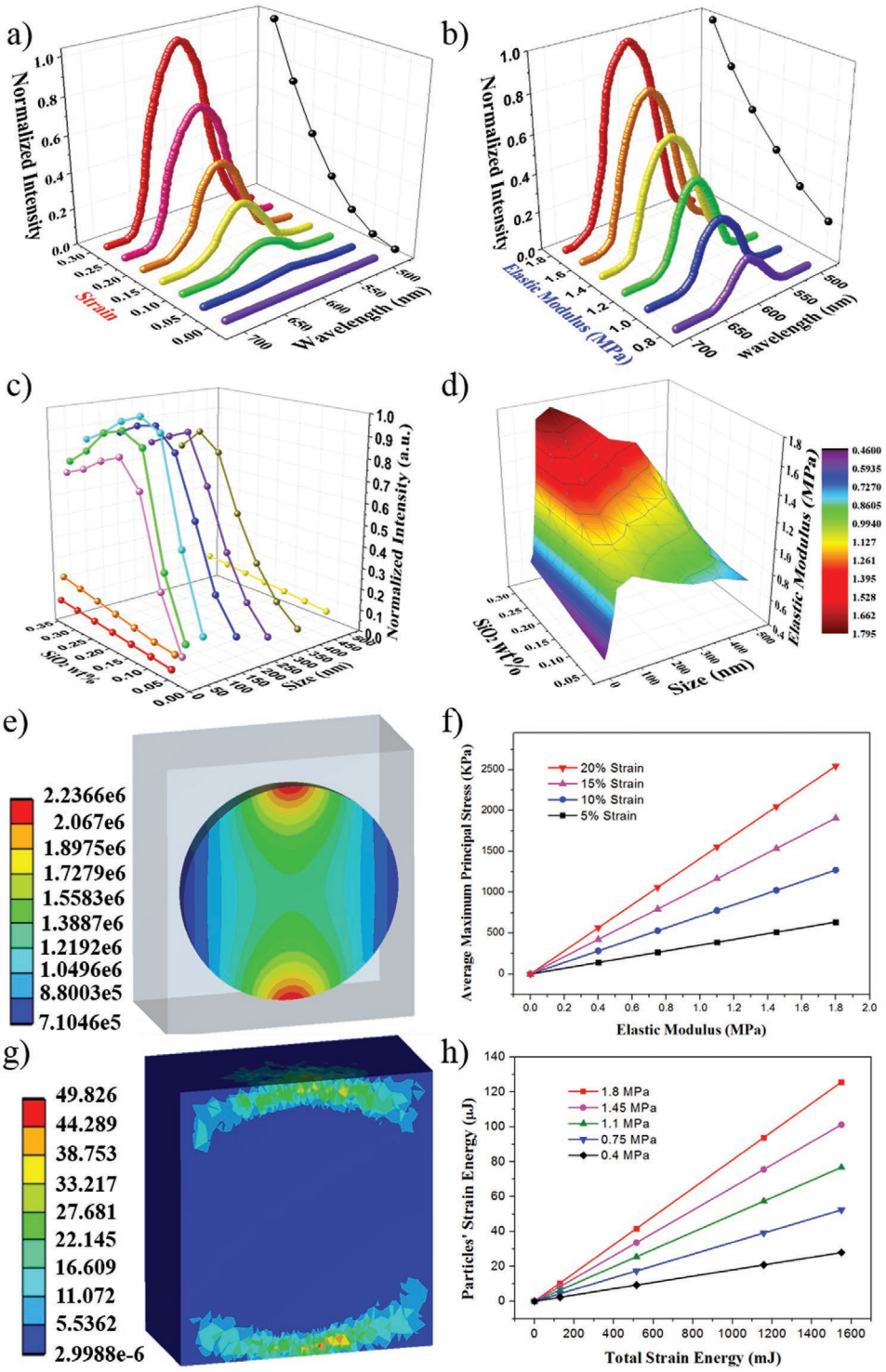

Figure 2. Experimental results and solid mechanics FEA for sensitive ML. a,b) The luminescence behaviors with different strain (a) or elastic modulus (b). c,d) SiO_2 nanoparticles doped (with different size or concentration) modifications define various luminescence sensitivity (c) and elastic modulus (d). e) FEA for static stress distribution on a ZnS spherical microparticle model. f) The simulation result of average maximum principal stress with elastic modulus. g) FEA for strain energy distribution of matrix around the ZnS spherical microparticle model. h) The simulation result of strain energy ratio on ZnS spherical microparticle model.

nanoparticle size is less than 100 nm, the intensity and elasticity modulus decrease. There are many references reported that elasticity modulus of nanoparticle–polymer composites is the result of a combination of particle size, particle loading, and interphase effects.[28,29] And the hardness and Young's modulus of different size SiO_2 nanoparticles can be different.[30]

FEA for static stress distribution on a ZnS spherical microparticle model, shown in Figure 2e, reveals that the maximum principal stress distributes mainly at the poles of the ZnS sphericity and vertical stretch direction. The model includes two components, the ZMPs and matrix. Matrix presents the composite of SiO_2 and PDMS. Figure 2f,h is obtained by sweeping the parameters of matrix elasticity modulus and strain in FEA. Figure 2f shows that the average maximum principal stress is proportional linear function with elastic modulus and strain. (Further detailed results of FEA are provided in Figure S5, Supporting Information.) The maximum principal stress is proportional to the strain of the model; with same strain, principal stress is proportional to the modulus of matrix. The threshold strain for ZMPs is about 1 MPa.[31] Figure 2g presents the strain energy distribution of matrix and the ZnS sphericity by FEA. The matrix absorbs most of the energy, which has no contribution to ML. The strain energy of ZnS particles to the total strain energy is very small. The strain energy is proportional linear function with total strain energy for various elastic modulus matrixes, as the simulation plot result is shown in Figure 2h. By increasing the elastic modulus of the matrix, the ratio of the strain energy of the ZnS particles increases accordingly. Via doping nano-SiO_2 particles into the PDMS, the elastic modulus of matrix can be regulated quantitatively, then modify ZMPs PDMS composite's mechanical properties and the ML performance.

Printing is advantaged in the vast material adoptability,[32] facile,[33] high individual pixel resolution,[34] and massive production.[35] We prepared ZMPs nano-SiO_2 PDMS ink and applied it to direct-write printing process, as **Figure 3**a illustrated. The rheology of the ink was optimized to print filaments with moderate aspect ratio, which ensures the entity of the patterned ML layer architecture and keeps the underlying layers with minimal deformation. Figure 3b provides the apparent viscosity (η) as a function of shear rate, the viscosity is in proportion to the ink concentration. The solid loading of different concentration (c) ranging from 55–85% was investigated (ML particles can hardly send out luminescence in PDMS when $c \leq 50\%$). The viscosity was dramatically increased at low shear rate when the ink concentration reached 85%. The exhibited highly shear thinning behavior guaranteed the ink flowing smoothly through the nozzle during printing. Figure 3c demonstrated their storage modulus (G') and loss modulus (G'') as a function of shear strain. As concentration below 85%, it was liquid-like response ($G' < G''$). On the contrary, the ink with of 85% solid loading exhibited a storage modulus plateau that exceeded loss modulus by almost an order of magnitude at strain lower than shear yield strain (≈0.5%), which therefore ensured a solid-like nature in the quiescent state. Thus, the most desired rheological behavior due to its high viscosity under low shear rate, the shear thinning behavior, and the solid-like response ($G' > G''$) under low shear strain is the inks of 85% concentration. With various M^{2+}(Mn/Cu) doped, the ZMPs could be approached the printed patterns with different ML color, such as green, orange, and blue, as Figure 3d illustrated. The thickness of printed patterns also impacted ML intensity. As shown in Figure 3e, the ML intensity aggrandized following pattern thickness and reached to sluggish after 200 µm or thicker. With increased opacity, thick patterns will block the luminescence. The response time of the ML devices

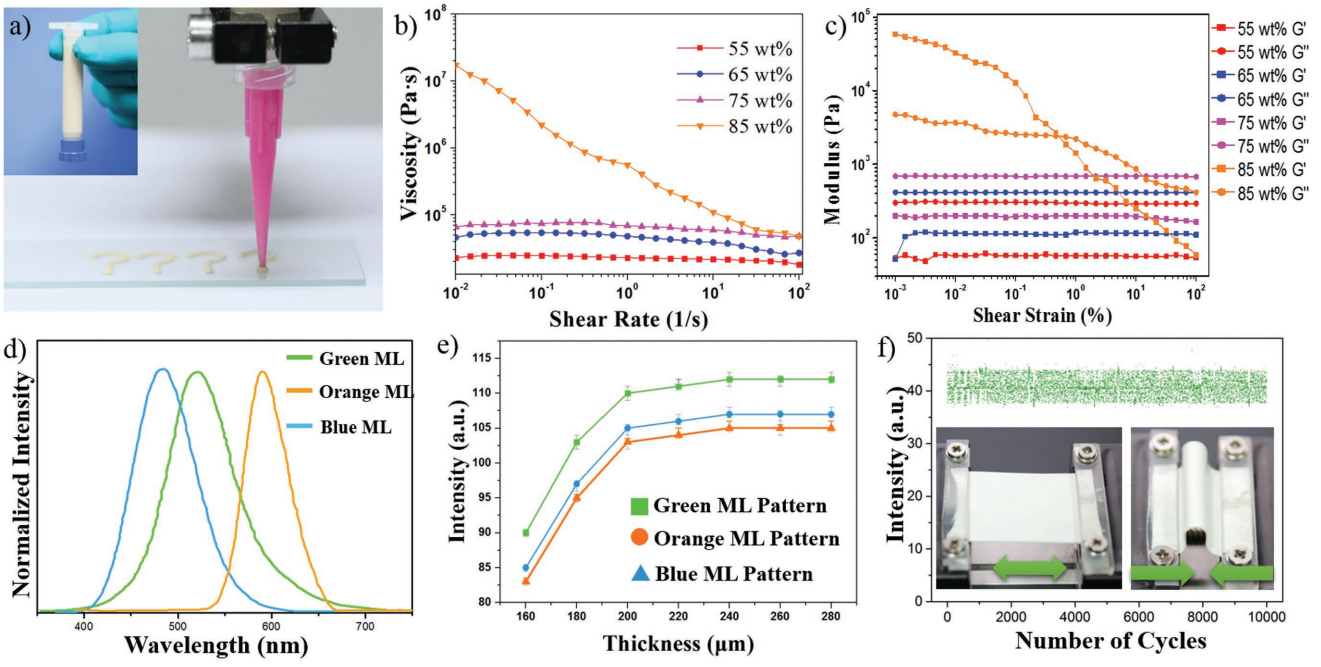

Figure 3. Printing process to achieve sensitive ML pattern devices. a) The doped ZMPs ink and direct writing prepared ML patterns. b) Ink viscosity (η) of nano-/microparticle-doped ML compounds uncured PDMS with different concentrations as a function of shear rate. c) Storage modulus (G') and loss modulus (G'') as a function of shear strain. d) Colorful ML can be achieved via different cation doped to ZnS. e) The ML behaviors depend on ZMPs pattern thickness. f) The repeatability and stability of the ML devices during 10 000 stretching–bending cycles. The durability tests were performed under a strain of 20% at a frequency of 2 Hz.

was exploited in Figure S6a,b in the Supporting Information. We tapped the ML film by a pen tip. The luminescence was recorded using fiber optic spectrometer and recorded the tap force with a force sensor. The luminescence response is consistent with the tap force. The full-width at half-maximum of the tap force is 60.5 ms, while the full-width at half-maximum of the luminescence is 65.2 ms. It should be noticed that the time resolution of fiber optic spectrometer is 8 ms, so the response time of the ML devices will be less than 8 ms. The full-width at half-maximum of luminescence is larger than the applied force due to the relaxation time of the phosphors. Figure 3f showed the films had excellent sensitivity and good repeatability during 10 000 bending and stretch cycles. The durability was tested under a strain of 20% at a frequency at 2 Hz.

Human skin possesses complicated mechanical properties. The movement of our muscles and joints causes the deformation of skin, and the strain of skin is different at different parts of human body. The facial skin exhibits less than 20% deformation and much weaker strain force compared with limbs and truncus.[36] Limited stretching and great fluctuations of different face skin areas require high efficiency at small strain. The critical requirement for adoptability of strain sensitive ML skin is the adjustable elasticity modulus to transmit strain stimulation onto ZMPs. We applied printed sensitive ML patterns functional film on human face to demonstrate the high performance for skin-driven ML exhibition. We use FEA to analyze the stress transmit from skin to ML films for designing skin-driven ML devices. **Figure 4**a–c shows the FEA stimulation of a printed ML patterns functional film attached on human facial skin. When the elastic modulus was set as 1 MPa (less than human skin elastic modulus, 2 MPa),[37] the static stress distribution on functional film will be lower than distribution on skin, Figure 4b. When the elastic modulus is set as 4 MPa (two times higher than human skin), the static stress mainly distributes on functional film (Figure 4c). As Figure 4d shown, the elastic modulus has a quadratic relation with ML intensity by experiments (the red plot) but a gentle linear relation with stress by FEA (the blue plot). Influence of the film thickness is discussed in Figure S9 in the Supporting Information. Balance with elastic modulus and flexibility, we print 200 µm thickness ML patterns and attach to a demonstrator facial skin. As Figure 4e–g presented, various punctuation marks with different ML color are attached on lips corner, canthus, and cheek, respectively. When the presenter twitch her lip's corner to right or left, the exclamation mark pattern will be lightened; and a laugh with open mouth drives double lighten exclamation, which expresses the augmented ecstatic emotion. The nictations will pull canthus skin and lighten the question mark pattern to augment query or confusion. The quotation marks on cheek will be launched with swelling cheek and present fetching cute smile. The active exhibition is presented in Movie S3 in the Supporting Information.

In conclusion, we designed facile nanoparticle-doped matrix modification architecture to enhance the sensitivity of flexible ML devices. Rigid ZMPs were dispersed into soft PDMS matrix. Optimal size and contains of SiO_2 nanoparticles doping were investigated to adjust the elasticity modulus of PDMS matrix for various flexible and sensitive scenes. Facilely fitting with human skin elasticity modulus, printed nanoparticle-doped matrix film can achieve skin (weak stimuli) driving ML, the photonic-skin phenomenon, which can be adopted to present fetching augmented animations expressions. The printable ML devices provide the large-scale fabrication for performing sensitive and stable luminescence response on deformations, and will be versatile on stress visualization, luminescent sensors, and micromotion manipulation auxiliary apparatuses. It may remarkably offer opportunity new expressions for human social interactions with reality augmented animation effectiveness.

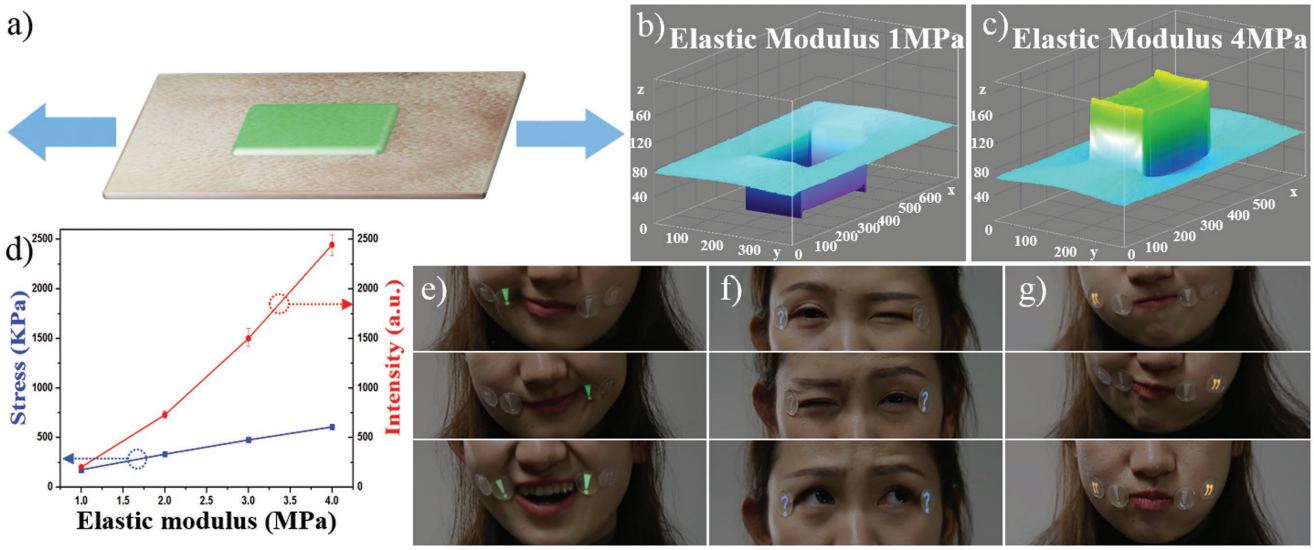

Figure 4. The skin driving ML exhibition. a) A ML film stretching FEA simulating on skin. b,c) The 3D representation of FEA for static stress distribution ML film with 1 MPa (half of human facial skin) elastic modulus attached skin (b), and 4 MPa (two times human facial skin) elastic modulus attached skin (c). d) The relation of elastic modulus corresponding to stress by FEA and ML intensity by experiments. The skin-driven various color ML response to lips corner e), canthus f), and cheek g) muscle movements.

Experimental Section

Preparation of the ZMPs: Detail of preparation is introduced in the Supporting Information.

Direct Writing of the ML Devices: The 85% SiO_2–ZnS:Mn/Cu^{2+}-doped PDMS ink was used. The micropattern was created using a 3-axis micropositioning stage. All the samples were cured at 80 °C for 0.5 h.

ML Measurements: A homemade measuring system was built to collect ML spectrum, and a mechanical motion platform was used to apply the strain levels. Light emissions were collected from the contact point by a spectrometer (Ocean Optics QE65pro) in the range of 200–900 nm. In the response time test, the tap force was measured by a pressure sensor (ATI Nano17). The details are introduced in the Supporting Information.

Supporting Information

Supporting Information is available from the Wiley Online Library or from the author.

Acknowledgements

X.Q. and Z.C. contributed equally to this work. X.Q. specially thanks for Yi Ding's great help. F.L. and Y.S. thank the National Nature Science Foundation of China (Grant Nos. 51773206, 51473172, and 51473173), the National Key R&D Program of China (Grant Nos. 2016YFB0401603, 2016YFC1100502, and 2016YFB0401100), and the "Strategic Priority Research Program" of the Chinese Academy of Sciences (Grant No. XDA09020000). These experiments were performed in the scope of approval by the Committee on the Use of Human Subjects and Institutional Review Board of Institute of Chemistry, Chinese Academy of Sciences, following informed signed consent from the particant.

Conflict of Interest

The authors declare no conflict of interest.

Keywords

direct writing, matrix manipulation, mechanoluminescence, nano-/microdopant, photonic skin

Received: January 13, 2018
Revised: February 12, 2018
Published online:

[1] R. Webb, A. Bonifas, A. Behnaz, Y. Zhang, K. Yu, H. Cheng, M. Shi, Z. Bian, Z. Liu, Y. Kim, W. Yeo, J. Park, J. Song, Y. Li, Y. Huang, A. Gorbach, J. Rogers, *Nat. Mater.* **2013**, *12*, 938.
[2] M. Belanger, Y. Marois, *J. Biomed. Mater. Res.* **2001**, *58*, 467.
[3] D. Lipomi, M. Vosgueritchian, B. Tee, S. Hellstrom, J. Lee, C. Fox, Z. Bao, *Nat. Nanotechnol.* **2011**, *6*, 788.
[4] V. Maheshwari, R. Saraf, *Angew. Chem., Int. Ed.* **2008**, *47*, 7808.
[5] B. Tee1, A. Chortos, A. Berndt, A. Nguyen, A. Tom, A. McGuire, Z. Lin, K. Tien, W. Bae, H. Wang, P. Mei, H. Chou, B. Cui, K. Deisseroth, T. Ng, Z. Bao, *Science* **2015**, *350*, 313.
[6] B. Chandra, R. Baghel, V. Chandra, *Chalcogenide Lett.* **2010**, *7*, 1.
[7] C. Xu, T. Watanabe, M. Akiyama, X. Zheng, *Appl. Phys. Lett.* **1999**, *74*, 1236.
[8] D. Olawale, T. Dickens, W. Sullivan, O. Okoli, J. Sobanjo, B. Wang, *J. Lumin.* **2011**, *131*, 1407.
[9] B. Chandra, C. Xu, H. Yamada, X. Zheng, *J. Lumin.* **2010**, *130*, 442.
[10] T. Sekitani, H. Nakajima, H. Maeda, T. Fukushima, T. Aida, K. Hata, T. Someya, *Nat. Mater.* **2009**, *8*, 494.
[11] T. Yokota, P. Zalar, M. Kaltenbrunner, H. Jinno, N. Matsuhisa, H. Kitanosako, Y. Tachibana, W. Yukita, M. Koizumi, T. Someya, *Sci. Adv.* **2016**, *2*, e1501856.
[12] C. Wang, D. Hwang, Z. Yu, K. Takei, J. Park, T. Chen, B. Ma, A. Javey, *Nat. Mater.* **2013**, *12*, 899.
[13] D. Akinwande, N. Petrone, J. Hone, *Nat. Commun.* **2014**, *5*, 5678.
[14] X. Wang, R. Ling, Y. Zhang, M. Que, Y. Peng, C. Pan, *Nano Res.* **2017**, *11*, 1967.
[15] B. Qin, H. Chen, H. Liang, L. Fu, X. Liu, X. Qiu, S. Liu, R. Song, Z. Tang, *J. Am. Chem. Soc.* **2010**, *132*, 2886.
[16] Z. Li, Z. Zhu, W. Liu, Y. Zhou, B. Han, Y. Gao, Z. Tang, *J. Am. Chem. Soc.* **2012**, *134*, 3322.
[17] H. Gu, L. Bi, Y. Fu, N. Wang, S. Liu, Z. Tang, *Chem. Sci.* **2013**, *4*, 4371.
[18] Y. Li, J. Tang, L. He, Y. Liu, Y. Liu, C. Chen, Z. Tang, *Adv. Mater.* **2015**, *27*, 4075.
[19] L. Shi, L. Zhu, J. Guo, L. Zhang, Y. Shi, Y. Zhang, K. Hou, Y. Zheng, Y. Zhu, J. Lv, S. Liu, Z. Tang, *Angew. Chem., Int. Ed.* **2017**, *56*, 15397.
[20] X. Wang, H. Zhang, R. Yu, L. Dong, D. Peng, A. Zhang, Y. Zhang, H. Liu, C. Pan, Z. Wang, *Adv. Mater.* **2015**, *27*, 2324.
[21] S. Jeong, S. Song, K. Joo, J. Kim, S. Hwang, J. Jeong, H. Kim, *Energy Environ. Sci.* **2014**, *7*, 3338.
[22] J. Matinlinna, C. Y. K. Lung, J. K. H. Tsoi, *Dent. Mater.* **2018**, *34*, 13.
[23] S. Fu, X. Feng, B. Lauke, Y. Mai, *Composites, Part B* **2008**, *39*, 933.
[24] R. A. Pearson, A. F. Yee, *J. Mater. Sci.* **1991**, *26*, 3828.
[25] Y. Wong, L. Zhu, W. S. Teo, Y. Tan, Y. Yang, C. Wang, H. Chen, *J. Am. Chem. Soc.* **2011**, *133*, 11422.
[26] X. Song, T. Ding, L. Yao, M. Lin, R. Tan, C. Liu, K. Sokol, L. Yu, X. Lou, H. Chen, *Small* **2015**, *11*, 4351.
[27] Y. Ishigure, S. Iijima, H. Ito, T. Ota, H. Unuma, M. Takahashi, Y. Hikichi, *J. Mater. Sci.* **1999**, *34*, 2979.
[28] I. Rahman, V. Padavettan, *J. Nanomater.* **2012**, *2012*, 8.
[29] J. Jang, B. Bouveret, J. Suhr, R. F. Gibson, *Polym. Composite* **2012**, *33*, 1415.
[30] D. Guo, G. Xie, J. Luo, *J. Phys. D: Appl. Phys.* **2013**, *47*, 013001.
[31] B. Chandra, V. Chandra, P. Jha, V. Sonwane, *Phys. B (Amsterdam, Neth.)* **2016**, *491*, 12.
[32] W. Li, F. Li, H. Li, M. Su, M. Gao, Y. Li, D. Su, X. Zhang, Y. Song, *ACS Appl. Mater. Interfaces* **2016**, *8*, 12369.
[33] S. Chen, M. Su, C. Zhang, M. Gao, B. Bao, Q. Yang, B. Su, Y. Song, *Adv. Mater.* **2015**, *27*, 3928.
[34] M. Su, Z. Huang, Y. Huang, S. Chen, X. Qian, W. Li, Y. Li, W. Pei, H. Chen, F. Li, Y. Song, *Adv. Mater.* **2016**, *29*, 1605223.
[35] M. Gao, L. Li, W. Li, H. Zhou, Y. Song, *Adv. Sci.* **2016**, *3*, 1600120.
[36] H. Marcellier, P. Vescovo, D. Varchon, P. Vacher, P. Humbert, *Skin Res. Tech.* **2001**, *7*, 246.
[37] F. Khatyr, C. Imberdis, P. Vescovo, *Skin Res. Technol.* **2004**, *10*, 96.